

1 Main Manuscript for:

2 Cyclic and pseudo-cyclic electron pathways play antagonistic roles 3 during nitrogen deficiency in *Chlamydomonas reinhardtii*

4 Ousmane Dao^{1 *}, Adrien Burlacot^{2,3}, Marie Huleux¹, Pascaline Auroy¹, Gilles Peltier¹, Yonghua Li-
5 Beisson^{1*}

6
7
8 ¹Aix Marseille Univ, CEA, CNRS, Institute of Bioscience and Biotechnology of Aix Marseille, BIAM,
9 CEA Cadarache, Saint Paul-Lez-Durance, France

10 ²Department of Plant Biology, The Carnegie Institution for Science, Stanford, CA, 94305 USA

11 ³Department of Biology, Stanford University, Stanford, CA, 94305, USA

12
13 *Correspondence to: Yonghua Li-Beisson (yonghua.li@cea.fr) or Ousmane Dao
14 (ousmanedao17@yahoo.fr)

15 Author's Contributions:

16 Y.L-B., G.P., A.B., and O.D. conceived the study. O.D. performed most of the experiments. P.A. and
17 O.D. carried out biochemical experiments. M.H. and O.D. performed starch and lipid analysis. G.P.
18 supervised the MIMS experiments. O.D. drafted the manuscript with contributions from Y.L-B., A.B.
19 and G.P.

20
21
22 **ORCID IDs:** 0000-0002-7040-5770 (O.D), 0000-0001-7434-6416 (A.B.), 0000-0001-5098-1554 (M.H),
23 0000-0002-3376-6550 (P.A.), 0000-0002-2226-3931 (G.P.), 0000-0003-1064-1816 (Y.L.-B.).

24
25
26 **Competing Interest Statement:** There are no conflicts of interest.

27
28 **Classification:** Biological Sciences: Plant Biology

29
30 **Keywords:** Microalgae; Flavodiiron proteins; Cyclic electron flow; Triacylglycerol; Photosynthetic
31 control

32 This PDF file includes:

33
34
35
36 Main Text
37 Figures 1 to 5
38
39
40
41
42
43

Abstract (250 words)

Nitrogen (N) deficiency is a frequently encountered situation that constrains global biomass productivity. In response to N deficiency, cell division stops and photosynthetic electron transfer are downregulated, while carbon storage is enhanced. However, the molecular mechanism downregulating photosynthesis during N deficiency and its relationship with carbon storage are not fully understood. The Proton Gradient Regulator-like 1 (PGRL1)-involved in cyclic electron flow (CEF) and Flavodiiron proteins involved in pseudo-(CEF) are major players in the acclimation of photosynthesis. To determine the role of PGRL1 or FLV in photosynthesis under N deficiency, we measured photosynthetic electron transfer, oxygen gas exchange and carbon storage in the knockout of *Chlamydomonas* *pgrl1* and *flvB* mutants. Under N deficiency, *pgrl1* maintains higher net photosynthesis and O₂ photoreduction rates, while *flvB* shows similar responses compared to control strains. The amount of cytochrome *b₆f* was maintained at a higher level in *pgrl1*. The photosynthetic activity of *pgrl1 flvB* double mutants decreases in response to N deficiency similar to the control strains. Furthermore, the triacylglycerol content of *pgrl1* was twice higher than the controls under N deficiency. Taken together, our results suggest that in the absence of PGRL1, FLV-mediated O₂ photoreduction through PCEF maintains net photosynthesis at a high level, resulting in increased triacylglycerol biosynthesis. This study reveals that PGRL1 and FLV play antagonistic roles during N deficiency. It further illustrates how nutrient status can affect the regulation of photosynthetic energy production in relation to carbon storage and provides new strategies for improving lipid productivity in algae.

Significance statement

Nitrogen (N) deficiency, an often-encountered phenomenon in nature, triggers growth arrest and massive lipid accumulation in microalgae. The downregulation of photosynthesis is necessary to ensure cell viability. We demonstrate that a well-conserved protein in chlorophytes, the Proton Gradient Regulator-like 1 (PGRL1) is a key (down) regulator of photosynthesis. In its absence, cells exhibited sustained photosynthesis and over-accumulated lipids thanks to the Flavodiiron (FLV) protein. We propose that both PGRL1 and FLV, by having antagonistic roles in N deficiency, manage the redox landscape, carbon storage and biomass production. Our work revolves around the current paradigm of photosynthesis regulation during N deficiency and provides a new framework for improving lipid accumulation in microalgae for biotechnological purposes.

Introduction

Nitrogen (N) deficiency is one of the most harsh environmental situation that constrains global primary biomass productivity in all ecosystems (1–3). Under N deficiency, cell division and photosynthetic CO₂ assimilation are downregulated, the carbon and energy are used to synthesize starch and triacylglycerols (TAGs) (4–7). The downregulation of electron transfer reactions, together with a re-routing of the excess of reducing power towards carbon storage, prevents over-production of reactive oxygen species, thus ensuring cell fitness (8–12).

Due to the variability in their natural habitat, microalgae must constantly adjust the production of energy by photosynthesis to match the metabolic demand and have therefore developed a set of regulatory mechanisms to fine-tune electron transfer reactions. During photosynthesis, energy in the form of ATP and NADPH is mostly produced by the linear electron flow (LEF) (13). The balance of ATP and NADPH is essential for optimal CO₂ capture and metabolism to which cyclic electron flow (CEF) and pseudo-cyclic electron flow (PCEF) play a critical role (14–17). Two pathways of CEF around PSI have been described in the green microalga *Chlamydomonas reinhardtii* (*Chlamydomonas* hereafter), one involving the type II NADPH dehydrogenase (NDA2) (18), and the other the proton gradient regulator 5 (PGR5)/PGR-like 1 (PGRL1) proteins (19). Both CEF pathways reduce the plastoquinone (PQ) pool by using either NADPH or ferredoxin (Fd) as electron donor respectively (18, 20). CEF has been shown to take part in the acidification of thylakoid lumen through generating an extra proton motive force (*pmf*) in addition to the one produced by LEF (18, 19, 21, 22). PCEF mediated by Flavodiiron proteins (FLVs), by transferring electrons from Fd toward O₂, also contributes to the establishment of the *pmf* and therefore to the lumen acidification (23–25). The *pmf* is used to either (1) produce ATP (26), (2) trigger light energy quenching via a low luminal pH (27–29) or (3) repress electron transfer at the level the cytochrome *b₆f* complex through the photosynthetic control triggered by the low luminal pH (21, 30–32). Both CEF and PCEF have been shown to be critical under various conditions of light, CO₂ availability or sulfur deficiency, where both mechanisms have been found to play a synergistic role (14, 24, 25, 33, 34).

Despite the importance of CEF and PCEF in response to dynamic environments, little is known about their role during N deficiency. The role of NDA2-involved CEF have been recently addressed during CO₂-limiting photoautotrophic N deficiency and the lack of NDA2 was shown to impair the establishment of non-photochemical quenching (22). The role of PGRL1-PGR5 pathway has been investigated under mixotrophic N deficiency and the lack of PGRL1 was shown to decrease the rate of CEF and consequently TAG production (35). However, the role of PGRL1 during photoautotrophic N deficiency and the possible existence of interactions between carbon/energy sinks (TAG and starch) and (P)CEF pathways has not been explored so far. The latter appears particularly important considering that massive carbon reallocation occur under N deficiency (4). Fully understanding the role of these regulatory pathways and how they affect reserve formation is also needed towards engineering photosynthesis and improving lipid production in conditions of nutrient deficiency.

Here, we evaluated the contribution of PGRL1-mediated CEF in the regulation of photosynthesis during N deficiency and its interaction with carbon reserve accumulation in *Chlamydomonas* cells grown in photoautotrophic conditions in non-limiting CO₂ concentrations (using CO₂-enriched air), conditions which favor the accumulation of carbon reserves (7, 36, 37). By monitoring photosynthetic activity based on chlorophyll fluorescence and O₂ exchange rates measurements, we observed a continuous and high net and gross photosynthetic activity, elevated O₂ uptake and hyper-accumulation of TAGs in a PGRL1-deficient strain under N deficiency compared to the control strains. By characterizing mutants deficient in either PGRL1, FLVs or both we showed that FLVs, by maintaining a strong PCEF in the *pgrl1* mutant, allows maintaining high photosynthetic rates and high TAG accumulation. Finally, we discuss how modulating photosynthetic electron flow could constitute an efficient strategy to boost TAG production under nutrient deficiency.

Results

A PGRL1-deficient mutant showed sustained photosynthetic activity under N deficiency

To first assess the role of PGRL1 in the regulation of photosynthesis during photoautotrophic N deficiency, we simultaneously monitored chlorophyll fluorescence and O₂ exchange following a dark-light-dark transition in N-replete and N-deprived cells. We compared the photosynthesis efficiency of the PGRL1-deficient strain (*pgrl1* hereafter) with its control wild-type strain (137AH) and two complemented lines (19) (Fig. 1 and Supplemental Fig. S1 and S2). Under N replete condition, both chlorophyll fluorescence and net O₂ evolution patterns were mostly similar in *pgrl1* and control cells (Fig. 1 A, B, E and F). *pgrl1* exhibited higher O₂ uptake and gross O₂ production rates in the light as compared to control lines (Fig. 1B and F), as previously reported (14, 25). After 2 days of N

deficiency, the PSII operating yield measured in the light decreased by about 75% in the WT and only by 35% in *pgrl1* (Fig. 1 C, D, E and F; Supplemental Fig. S1C). As previously reported (5, 38) the dark respiration rate was stimulated in the WT under N deficiency, this effect being reduced in *pgrl1* (Supplemental Fig. S2 and S4). Conversely, *pgrl1* showed twice higher net O₂ evolution and light-dependent O₂ uptake as compared to the WT (Fig. 1 D and F). By using *pgrl1* complemented lines (19) we observed full recovery in the *pgrl1::PGRL1-2* and a partial recovery in *pgrl1::PGRL1-1* (Supplemental Fig. S1 and S2). The preservation of photosynthetic activity in *pgrl1* suggests that CEF contributes to repressing the activity of photosynthetic electron transfer under photoautotrophic N-deficiency.

Cyt *b₆f*, PsaD and FLVs accumulate to higher levels in *pgrl1* as compared to its control under N deficiency

The amount of photosynthetic proteins drops when Chlamydomonas cells undergo N deficiency under mixotrophic conditions (5, 39). However, this effect strongly depends on growth conditions, as the amount of photosynthetic proteins is maintained at high level when cells are grown under CO₂-limiting photoautotrophic conditions (22). By loading similar protein amounts, we observed detectable amount of PGRL1, NDA2, FLVA and FLVB proteins up to 48h of N deficiency although FLVs were found at lower amount compared to N-replete conditions (Fig. 2 A and B). A strong reduction in the amounts of Cyt *f*, PsaD, PsaC and PsaD subunits were observed when N deficiency was performed in non-limiting CO₂ photoautotrophic, thus indicating a reduction in the amounts of Cyt *b₆f*, PSII and PSI complexes (Fig. 2 A and B). We conclude from these analyses that N-limitation induces a strong decrease in most proteins involved in photosynthetic electron transport with the exception of the CEF proteins PGRL1 and NDA2.

To gain insights into the mechanisms behind the high photosynthetic activity in *pgrl1* during N deficiency, we compared the relative abundance of major proteins involved in photosynthetic complexes and in CEF and PCEF in the *pgrl1* and the WT during N deficiency (Fig. 2 C and D). Interestingly, we observed a higher accumulation of the PSI subunit PsaD and reduced degradation of Cyt *f* in *pgrl1* compared to the WT (Fig. 2 C and D). FLVA amount was found more abundant after 2 d of N deficiency despite a reduced level in N-replete in *pgrl1* compared to the WT (Fig. 2 C and D). It is worth noting that the hallmark of autophagy i.e. ATG8 was barely detectable in the mutant whereas it was highly induced in the WT under N deficiency (Fig. 2 C and D). All the other proteins tested accumulated to a similar amount in *pgrl1* and WT (Fig. 2 C and D). We conclude from this experiment that *pgrl1* mutant keeps a higher photosynthetic activity during N deficiency than the WT thanks to a lower decrease of the Cyt *b₆f* amount and higher accumulation of PSI and FLVs proteins.

FLV-mediated O₂ photoreduction drives photosynthesis in *pgrl1* under N deficiency

The above data (Fig. 1 and 2) suggest that PGRL1 is involved in the downregulation of PET, and that a light-dependent O₂ uptake mechanism is activated in *pgrl1* during N deficiency. We then questioned the nature of molecular actors involved in the increased O₂ uptake. As FLVs have been reported to be the main O₂ uptake mechanism in the light (24, 25, 40), we evaluated steady-state O₂ exchange rate in *pgrl1*, *flvB* as well as in the *pgrl1 flvB* double mutants (Fig. 3). In N-deficiency, the light-dependent O₂ uptake, was highly increased in *pgrl1* but strongly impaired in *flvB* and *pgrl1 flvB* mutants (supplemental Fig. S3 and S4B) which mirrors what has been reported for N-replete conditions (24, 25). Interestingly, while both O₂ uptake in the light and net O₂ production measured during steady-state photosynthesis remained high in *pgrl1*, no marked difference in gross or net O₂ exchange were detected between *flvB*, *pgrl1 flvB* and their respective control lines (Figure 3 A-C and supplemental Fig. S2 and S3). Immunoblot analyses showed similar accumulation of NDA2, Cyt *f*, PsaD, and ATG8 proteins in the *pgrl1 flvB* compared to controls under N replete and deficiency (Fig. 3D). Taken together, these data show that the absence of FLV-mediated PCEF in the *pgrl1* background restores the effect of N limitation observed in control strains. We conclude that FLV-mediated PCEF by maintaining photosynthetic electron transfer reactions in *pgrl1* allows net photosynthesis to be maintained at a high level during N deficiency.

***pgrl1* over accumulates TAGs under N deficiency**

Emerging literature suggests that alterations of energy management pathways affect not only biomass production but also its composition (16, 17, 36, 41). Starch and TAGs are major forms of carbon storage in Chlamydomonas during N deficiency. Since *pgrl1* mutant shows stronger net photosynthetic rate, we measured its ability to accumulate storage compounds. Starch accumulation was similar in *pgrl1* and control lines under both N replete and deficiency (Fig. 4A; Supplemental Fig. S5, S7 A and B). In contrast, thin-layer chromatography (TLC) revealed twice more TAG accumulation in *pgrl1*

compared to the control lines under N deficiency whereas no difference was observed under N-replete condition (**Fig. 4B; Supplemental Fig. S5 and S7 C and D**). Lipid droplet imaging confirmed the observation of TAG quantification by TLC (**Fig. 4C**). To determine whether the increase in TAG is due to membrane lipid remodeling or to an improved *de novo* fatty acid biosynthesis in the chloroplast, we quantified total fatty acids by gas chromatography coupled to a mass spectrometer (GC-MS). We observed a net increase in total fatty acids in *pgrl1*, suggesting an increase in *de novo* fatty acid biosynthesis (**Supplemental Fig. S6**).

We then evaluated whether the changes in photosynthesis and TAG amount affect biomass accumulation, we followed changes in cell volume for 6 d during N deficiency. Cell volume is used here as a proxy for biomass accumulation. The cell volume increased twice faster in the *pgrl1* compared to the control lines (**Supplemental Fig. 5A**). We conclude from above experiments that the higher photosynthetic activity in *pgrl1* results in increased biomass and TAG productivity under N deficiency.

We then analyzed starch and TAG amount in *flvB* as well as *pgrl1 flvB* double mutants before and under N deficiency (**Supplemental Fig. S7**). Similar to the observations on photosynthetic activity, the *pgrl1 flvB* double mutant accumulated similar amounts of TAG and starch as compared to control strains either in N replete or N limited conditions (**Supplemental Fig. S7I-L**). Intriguingly, under optimal growth but not under N deficiency, the *flvB* single mutants accumulated much higher amount of starch than WT (**Supplemental Fig. S7E**) and accumulated lower amounts of TAG under N deficiency (**Supplemental Fig. S7H**). These data indicate that modifying regulatory mechanisms of photosynthetic electron transfer reactions strongly affects carbon storage in both quality and quantity (**Fig. 1 and 2**).

We conclude that during phototrophic N-deficiency, photosynthetic electron flow mediated by FLVs allows to drive photosynthetic TAG accumulation while PGRL1 tends to constrain it, likely via an activation of photosynthetic control. We propose that both PGRL1 and FLVs, by having an antagonistic role in N-deprivation, manage the redox landscape, carbon storage and biomass production.

Discussion

The ability of microalgae to coordinate their energy production to meet the metabolic demand is crucial for their survival in a constantly fluctuating environment. Mechanisms involved in photosynthesis regulations have been abundantly studied in response to light or CO₂ levels, but not much is known during nutrient deficiency when a massive re-orientation of metabolic pathways occur. In the absence of N, the major cellular energy sinks (cell division, protein biosynthesis and photosynthetic CO₂ fixation) are restricted whereas the carbon and energy are stored as TAGs or starch. Moreover, the photosynthetic electron transfer (PET) is downregulated to match the demand and maintain cell viability. In this study, we demonstrated that PGRL1 is involved in the downregulation of PET during N deficiency. This down-regulation likely operates via the photosynthetic control mechanism (see below for details). Lack of PGRL1 resulted in sustained efficient photosynthetic activity after 2 d of N deficiency. We have further shown that the release of photosynthetic control in *pgrl1* mutants resulted in higher FLVs-mediated PCEF. By channeling excess electrons toward O₂, PCEF prevents PSI acceptor side-limitation, allows maintaining PET at high level and favors high TAG accumulation. A schematic diagram explaining the role of PGRL1 in the downregulation of photosynthesis and metabolic consequences of its absence during N deficiency is presented in **Fig. 5**.

PGRL1-involved CEF contributes to photosynthetic control during N deficiency

Unlike in higher plants (21, 42–44), the photosynthetic control mechanism has been poorly studied in microalgae. The term ‘photosynthetic control’ refers to mechanisms that restrict the reactions of PET during the steady-state photosynthesis mostly occur in response to environmental fluctuations (31, 44). The Cyt *b₆f* is considered as the central hub for controlling PET between PSII to PSI and prevents the over reduction of P700 (44, 45). This is achieved either by slowing down the turnover rate (conductance) of the Cyt *b₆f* triggered by the acidification of the thylakoid lumen (44) followed (or not) by the selective autophagy of Cyt *b₆f* (39). In addition to Cyt *b₆f*, the PGRL1-PGR5-dependent CEF was shown to contribute to the photosynthetic control in higher plants (21, 43, 46) and lately in microalgae (19, 47–50). However, a recent work in *Chlamydomonas* reported that PGRL1 only slightly contribute to the luminal proton generation and that the *pgrl1* displayed similar proton gradient to the WT during photoautotrophic N deficiency under CO₂ limiting conditions (22). Our work shows that impairing the accumulation of the PGRL1 removes a bottleneck of photosynthetic electron flow during N deficiency under non-limiting CO₂ conditions (**Fig. 1 and 3; Supplemental Fig. S1 and S2**). Similar observations were reported under sulphur deprivation where deletion of PGRL1 or PGR5 resulted in

sustained linear electron flow toward H₂ production in *Chlamydomonas* (19, 49). The contribution of PGRL1 in the photosynthetic control is likely through the acidification of lumen that will exert a backpressure on Cyt *b₆f* conductance, slowing down the electron transfer toward plastocyanin. However, further works will be required to shed light on the exact participation of PGR5/PGRL1 in the photosynthetic control. Recently, PGR5 (which interacts with PGRL1 during the CEF (43) was shown to be required for efficient Q cycle through the reduction of the heme-*c_i* in the *b₆f* using reduced ferredoxin (50). The operation of the Q cycle is crucial for lumen acidification to trigger the onset of photosynthetic control (51–53). By doing so, PGRL1-PGR5 connects the stromal redox poise to the *b₆f*-dependent photosynthetic control.

FLVs become predominant in the absence of PGRL1-mediated cyclic electron flow

So far, a few studies reported a compensation mechanism between PGRL1 and FLVs during algal adaptation to high light or low-CO₂ conditions (14, 25). Under high light or low-CO₂ conditions, the increased activity of FLVs in the PGRL1-deficient strain had no significant improvement on the net photosynthesis but rather FLVs serve either as a safety valve of excess electrons or to balance ATP/NAD(P)H by generating more *pmf* (14, 25). Similar compensation has also been observed in higher plants where orthologous expression of FLVs rescues the *pgr5* mutants phenotype without further improvement photosynthesis (46, 54) although some level of increased biomass where measured in WT Arabidopsis expressing FLVs under light fluctuations thanks the protective role of FLVs in these conditions (55). In contrast, our results suggest that under N deficiency, FLVs and PGRL1 have an antagonistic role. Indeed, the increased activity of FLVs in the PGRL1-deficient strain resulted in higher net photosynthesis and TAG accumulation than in the WT (**Fig. 3D and 4B**), which shows that rather than compensating each other, PGRL1 is indirectly controlling the activity of FLVs by limiting the electron flow. Our observation of the sustained accumulation of Cyt *b₆f* and increased accumulation of PSI in the PGRL1-deficient strain under N deficiency (**Fig. 2C**) could be explained by the strong activity of FLVs draining electrons from the photosynthetic chain thereby releasing the over-reduction pressure and preventing PSI from damage. However, we were expecting that removal of both PGRL1 and FLVs should have more severe consequences on cell physiology and metabolism. Instead, we observed similar photosynthetic activity and TAG biosynthesis in the *pgr1 flvB* double mutants as their control strains (**Fig. 3 and supplemental Fig. S7**), i.e. the additional removal of FLVs suppressed the phenotype of PGRL1-deficient strain. The WT-like phenotype of *pgr1 flvB* double mutants further supports our conclusion that PGRL1 and FLV are antagonist during N deficiency. A third pathway taking over could explain this WT-like phenotype of the double mutant *pgr1 flvB*. The NDA2 pathway or chloroplast-mitochondria electron flow (CMEF) could be good candidates. NDA2 protein level was shown to increase during air photoautotrophic N deficiency and also the CEF rate in *Chlamydomonas* was decreased by 50% in *nda2* mutants (22). However, we observed a similar protein level of NDA2 in the *pgr1 flvB* as their control lines (**Fig. 3C and Supplemental Fig. S4D**). Nevertheless, the protein level might not always correlate with the activity and other regulatory mechanisms (e.g., phosphorylation or redox regulation) can modulate enzyme activity. However, the high rates of respiration in the dark in N-deprived WT and *pgr1 flvB* double mutants (**Fig. 1 and Supplemental Fig. S3 and S4A**) is a good indication that mitochondria is strongly active and likely reflects a strong CMEF, which would take over CEF and PCEF in N-deprived conditions. Altogether, we conclude that FLVs act as a major driving force leading to the increased net photosynthesis in *pgr1* under N deficiency (**Fig. 3**).

Relationship between cellular redox landscape and carbon storage

A major biotechnological challenge in algal domestication for biofuel is the low lipid productivity. In *Chlamydomonas* and many other microalgae, starch and TAG massively accumulate but mostly under stress conditions in particular N deficiency when cell division stops and productivity is impaired. Considerable efforts have focused on the study of the molecular mechanisms behind the onset of reserve accumulation by monitoring omics responses to a stress (5, 56–59), or focused on specific steps of fatty acid and TAG biosynthesis, which have resulted in some limited improvement in productivity (60, 61). Improving productivity requires a better understanding of the crosstalk between photosynthetic carbon fixation, environmental signals and the redox balance, which all govern reserve accumulation (62–64). Here by studying mutants affected in CEF and PCEF, we explored the relationships between the cellular redox status and carbon storage. The increased accumulation of TAG but not starch observed in the PGRL1-deficient strain under N deficiency (**Fig. 4 A and B**) is due to an increase in *de novo* biosynthesis in the chloroplast as evidenced by the observed increase in total fatty acids (**Supplemental Fig. S6**). The increase in TAG amount is a consequence of the continuous production of NADPH and ATP through PCEF in the PGRL1-deficient strain under nitrogen

deficiency. By alleviating the limitation of the acceptor side of PSI, PCEF released the over-reduction pressure of the photosynthetic chain, thereby sustaining the PET reactions. In line with our finding, the *Chlamydomonas pgd1* mutants (e.g. *Plastid galactoglycerolipid degradation 1*) with reduced LEF rate are shown to produce less TAG under N starvation (11, 65). The report that the *pgr1* mutant made less TAG than WT under mixotrophic conditions (66) is not surprising. It is well known that the bioenergetics of *Chlamydomonas* under photoautotrophic conditions differ from mixotrophic conditions (67–69). The presence of acetate can drastically affect cellular bioenergetics level i.e. its uptake consumes ATP and its metabolism produces NADH, therefore further favoring oil synthesis (67, 68, 70, 71).

Moreover, in addition to higher TAG amount, we also observed higher biomass (cell volume) in the PGRL1-deficient strain during N deficiency (**Supplemental Fig. 5A**). This high biomass can be interpreted by the combined increased of photosynthetic activity (**Fig. 1**), TAG biosynthesis (**Fig. 4**) and reduced autophagy as indicated by the amount of ATG8 (**Fig. 2**). Here we show that removing the photosynthetic control mediated by PGRL1 allows the FLVs-mediated PCEF to massively take part in the energization of the *de novo* fatty acid biosynthesis pathway resulting in improved TAG biosynthesis and double TAG productivity. Taken together, our data highlight the importance of energetic balance on carbon reserve formation for biomass production and for altering biomass composition. Rewiring the alternative photosynthetic electron flows opens new possibilities in fine tuning algal productivity and the organic compounds they are producing.

Materials and methods

Growth conditions and strains

The *pgr1* from the background 137AH, its two complementing strains, *flvB* mutants from the background CC-4533 and the double mutants *pgr1 flvB* were previously described (19, 24, 25). Cells were routinely cultivated in an incubation shaker (INFORS Multitron pro) maintained at 25°C, with 120 rpm shaking and constant illumination at 50 $\mu\text{mol m}^{-2} \text{s}^{-1}$. Fluorescent tubes delivering white light enriched in red wavelength supplied lightings in the INFORS. All experiments were performed under photoautotrophic condition with minimum medium with or without nitrogen source (MM and MM-N) buffered with 20 μM MOPS at pH 7.2 in air enriched with 1% CO_2 . Due to cell aggregation (*pgr1*) that prevent accurate cell counting, total cellular volume was measured using a Multisizer 4 Coulter counter (Beckman Coulter) and the different strains were diluted to reach a similar cellular concentration before N deficiency experiments.

Measurement of chlorophyll fluorescence using a Pulse Amplitude Modulation (PAM)

Chlorophyll fluorescence was measured using a PAM fluorimeter (Dual-PAM 100, Walz GmbH, Effeltrich, Germany) on the MIMS chamber as described in (40) using green actinic light (1250 $\mu\text{mol photon m}^{-2} \text{s}^{-1}$, green LEDs). Red saturating flashes (8,000 $\mu\text{mol photons m}^{-2} \text{s}^{-1}$, 600 ms) were delivered to measure the maximum fluorescence (FM) every 30 s (before and upon actinic light exposure). The maximum PSII quantum yield was calculated as $F_v/F_m = (F_m - F_0)/F_m$ where F_0 is the basal fluorescence obtained with the measuring light and F_m the fluorescence emitted after saturating pulse (72). PSII operating yield (Φ_{PSII}) was calculated as $\Phi_{\text{PSII}} = (F_m' - F_s)/F_m'$ with F_m' the fluorescence value after saturating pulse, F_s the stationary fluorescence during actinic light exposure.

O₂ exchange measurement using Membrane Inlet Mass Spectrometry (MIMS)

O₂ exchanges were measured in the presence of [¹⁸O]-enriched O₂ using a water-jacketed, thermoregulated (25°C) reaction vessel coupled to a mass spectrometer (model Prima ΔB; Thermo Electronics) through a membrane inlet system (73). The cell suspension (1.5 mL) was placed in the reaction vessel and bicarbonate (10 mM final concentration) was added to reach a saturating CO₂ concentration. One hundred microliters of [¹⁸O]-enriched O₂ (99% ¹⁸O₂ isotope content; Euriso-Top) was bubbled at the top of the suspension just before vessel closure and gas exchange measurements. O₂ exchanges were measured during a 3-min period in the dark, then the suspension was illuminated at 1250 $\mu\text{mol photons m}^{-2} \text{s}^{-1}$ for 5 min using green LEDs followed by 3-min in the dark. Isotopic O₂ species [¹⁸O¹⁸O] ($m/e = 36$), [¹⁸O¹⁶O] ($m/e = 34$), and [¹⁶O¹⁶O] ($m/e = 32$) were monitored, and O₂ exchange rates were determined (73). Argon gas was used to correct O₂ exchange measured by the spectrometer as described in (73).

All others methods are described in **SI Materials and Methods**.

Acknowledgments

O.D. thanks The French Atomic Energy and Alternative Energy Commission (CEA) for a PhD scholarship. G.P. and Y.L.-B. acknowledge the continuous financial support of CEA (LD-power, CO2Storage). A.B. acknowledges the support from the Carnegie Institution for Science. We thank Bertrand Legeret for maintaining the HelioBiotec lipidomics platform and thank Mallaury Cabanel for assistance in performing immunoblot. We also acknowledge the ZoOM microscopy facility.

Figures

Figure 1. *pgrl1* showed sustained photosynthesis after 2 d of N deficiency.

A-C, Chlorophyll fluorescence was measured using a Dual-PAM during the dark-light-dark transition from N-replete (**A**) and N-deficient (**B**) conditions.

D-F, O₂ exchange rates were measured using a MIMS in the presence of [¹⁸O]-enriched O₂. Net O₂ evolution (green) was calculated as gross O₂ production (blue) – gross O₂ uptake (red).

E, PSII quantum yield before and after 2 d of N deficiency. PSII (Y) was measured using green actinic light (1250 μmol photon m⁻² s⁻¹, green LEDs) and calculated as ΦPSII = (F_M' - F_s) / F_M' with F_M' the fluorescence value after saturating pulse, F_s the stationary fluorescence during actinic light exposure. Asterisks represent statistically significant differences compared to the control 137AH (* p<0.05, ** p<0.01 and *** p<0.001) using one-way ANOVA.

F, The Net O₂ production before and after 2 d of N deficiency in the wild-type 137AH, *pgrl1* and the complemented lines *pgrl1::PGRL1-1* and *pgrl1::PGRL1-2*.

G, Immunoblot analysis of PGRL1 accumulation in the wild-type 137AH, *pgrl1* and the complemented lines. L30 antibody was used as a positive control. Coomassie blue staining was used as the loading control. Protein samples were obtained from 2 d N-starved cells.

Wild type 137AH, *pgrl1*, *pgrl1::PGRL1-1* and *pgrl1::PGRL1-2* N-replete cells cultivated photoautotrophically with 1% CO₂ in air under continuous light (50 μmol photons m⁻² s⁻¹) were transferred into N-free media for 2 d prior to measurements. Shown are an average of at least three biological replicates ± SD.

Figure 2. *pgrl1* accumulated more cytochrome Cyt *b₆f* and PSI during N deficiency.

A, Immunodetection of photosynthetic proteins in the wild-type 137AH during N deficiency. Cells were harvested at 0, 16, 24, 40 and 48 h of N deficiency. Total proteins were extracted from the same cell number (20 million of cells) to quantitatively follow changes in specific protein amounts. Shown are representative images of three biological replicates. We validated our quantitative analysis by showing unchanged accumulation of the housekeeping α-tubulin protein and the timely induction of ATG8 autophagy protein despite the gradual degradation of total cellular proteins as shown by Coomassie staining during N deficiency.

B, Heatmap showing the abundance of proteins during N deficiency in the WT cells. The time 0 (N replete) was used for normalization. The color scale is shown in the right. Data are average of at least two biological replicates.

C, Immunodetection of photosynthetic proteins in the wild-type 137AH and *pgrl1* during N deficiency. Total proteins were extracted from cells harvested at 0, 8, 22, 30 and 50 h of N deficiency. Samples were loaded at equal total protein amounts as shown by Coomassie blue staining. Shown are representative images of three biological replicates.

D, Heatmap showing the proteins abundance during N deficiency in the *pgrl1* cells. The data from different time points were normalized to the WT protein amount. The color scale is shown in the right. Data are average of at least two biological replicates.

Figure 3. The photosynthesis in *pgrl1* is driven by FLV-mediated O₂ photoreduction under N deficiency.

A, Gross O₂ uptake measured between 5-7min as shown by the supplemental figure 3B.

B, Gross O₂ production measured between 5-7min as shown by the supplemental figure 3B

C, Net O₂ production measured between 5-7min as shown by the supplemental figure 3B

D, Immunodetection of photosynthetic protein in *pgrl1 flvB* and their control lines.

O₂ exchange rates were measured using a MIMS in the presence of [¹⁸O]-enriched O₂. Net O₂ evolution (green) was calculated as gross O₂ production (blue) – gross O₂ uptake (red). Total proteins were extracted from N-replete and 2 days N-deprived cells and samples were loaded at equal total proteins amounts as shown on Coomassie blue staining. Cells cultivated photoautotrophically with 1% CO₂ in air under continuous light of 50 μmol photons m⁻² s⁻¹ were transferred into N-free media for 2 days prior to measurements or sampling for immunoblot. Shown are an average of at least three biological replicates ± SD. Asterisks represent statistically significant difference compared to the WTs (* p<0.05, ** p<0.01, *** p<0.001 and **** p<0.0001) using one-way ANOVA.

Figure 4. *pgrl1* over accumulated TAGs under N deficiency

A, Starch amount.

B, TAG amount.

C, representative images of confocal microscopy observation of lipid droplet stained with Bodipy dye. Pseudo-colors were used: BODIPY-stained LDs in yellow, chlorophyll autofluorescence in red. DIC: differential interference contrast. Scale bar = 5 μ m.

Cells cultivated photoautotrophically with 1% CO₂ in the air under continuous light of 50 μ mol photons m⁻² s⁻¹ were transferred into N-free media for 2 d prior to sampling for starch and TAG or confocal imaging. Asterisks represent statistically significant difference compared to the control 137AH (* $p < 0.05$, ** $p < 0.01$ and *** $p < 0.001$) using one-way ANOVA.

Figure 5. Schematic diagram on the role of PGRL1 in the downregulation of photosynthesis and metabolic consequences of its absence during N deficiency

We proposed that PGRL1-mediated CEF is involved in the downregulation of photosynthesis during N deficiency through the Cyt *b6f*-dependent photosynthetic control (black arrow). In the absence of PGRL1, FLVs-mediated PCEF is strongly induced to drive the photosynthetic electron transfer. As a result, excess photosynthetic electrons are diverted toward fatty acid and triacylglycerol biosynthesis (* out of the chloroplast). The red arrows show the pathways upregulated in the PGRL1-deficient strain compared to the WT (gray arrows).

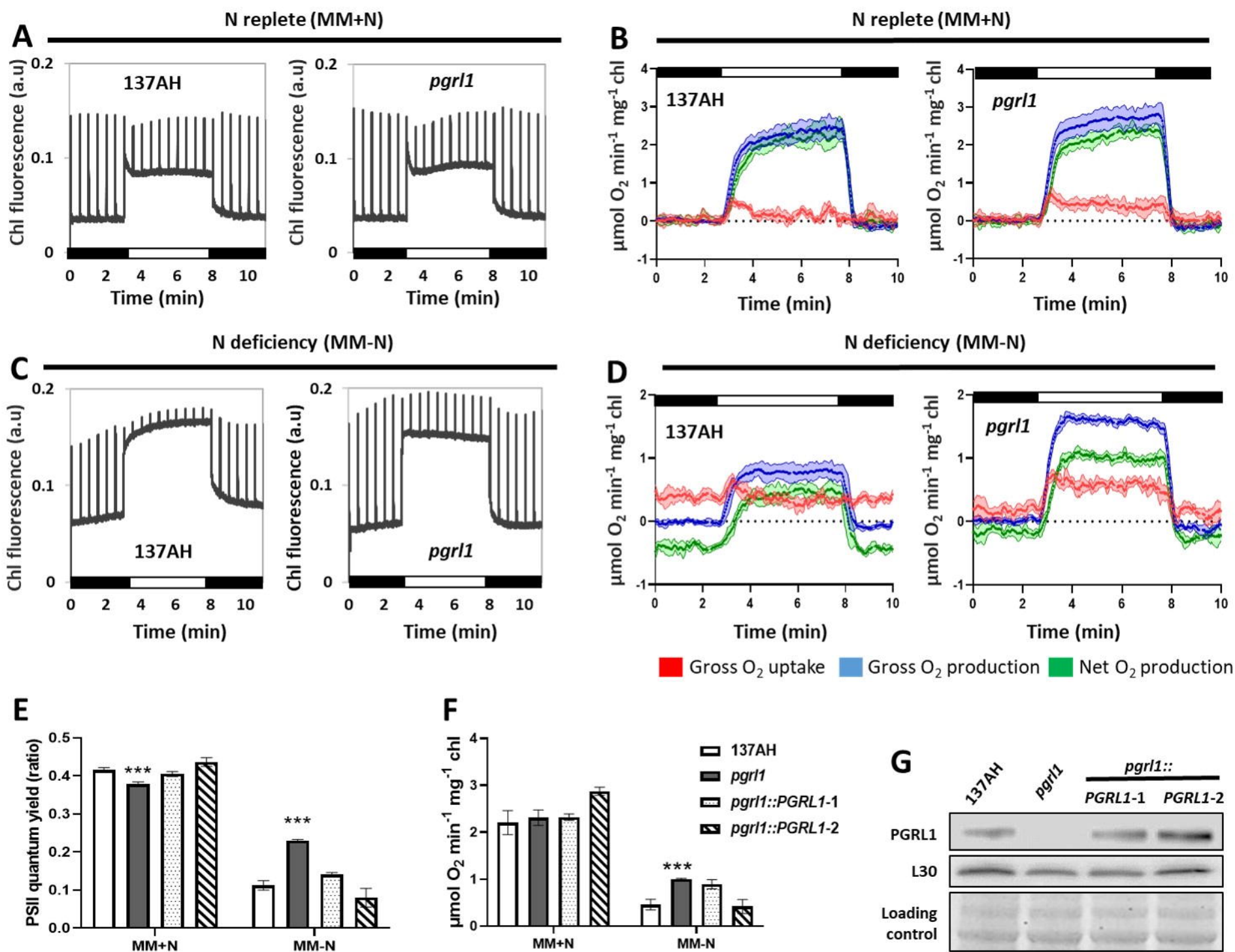
Reference

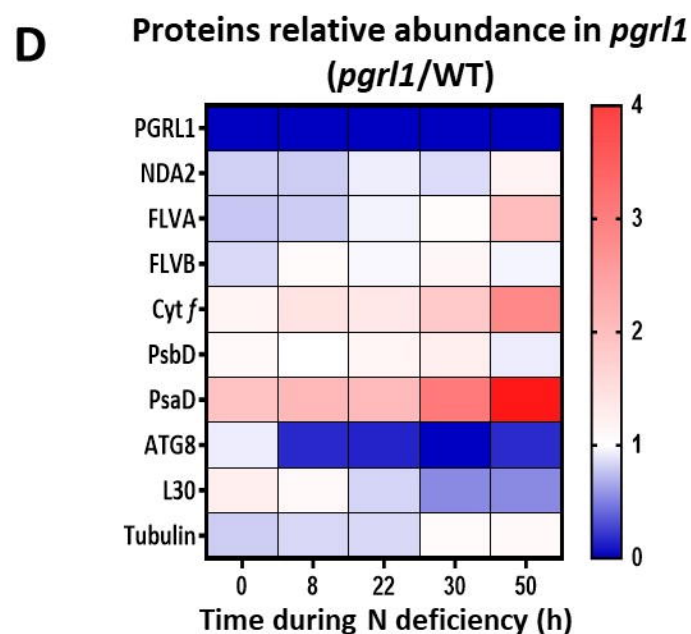
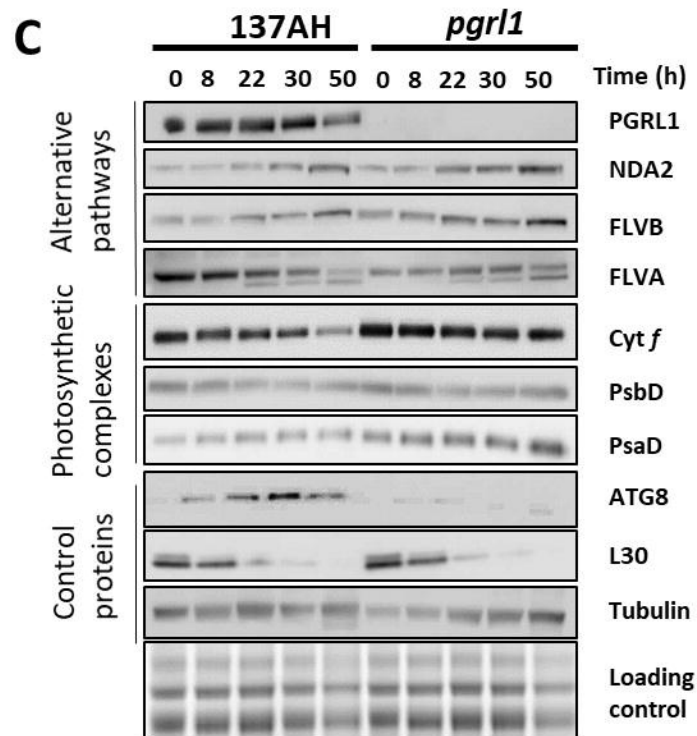
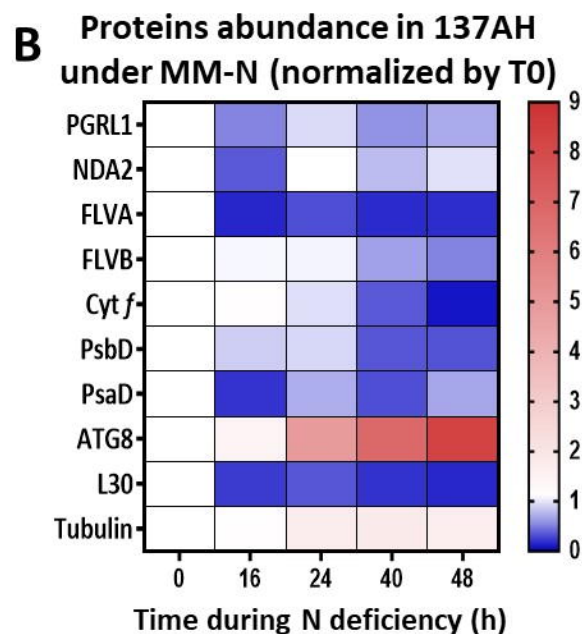
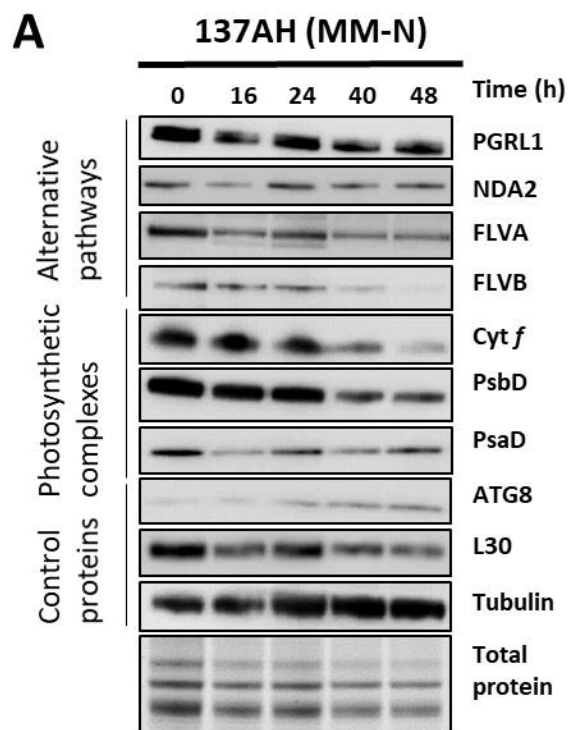
1. P. M. Vitousek, R. W. Howarth, Nitrogen limitation on land and in the sea: How can it occur? *Biogeochemistry* **13**, 87–115 (1991).
2. D. S. LeBauer, K. K. Treseder, Nitrogen limitation of net primary productivity in terrestrial ecosystems is globally distributed. *Ecology* **89**, 371–379 (2008).
3. E. Du, *et al.*, Global patterns of terrestrial nitrogen and phosphorus limitation. *Nat. Geosci.* **13**, 221–226 (2020).
4. M. Siaut, *et al.*, Oil accumulation in the model green alga *Chlamydomonas reinhardtii*: characterization, variability between common laboratory strains and relationship with starch reserves. *BMC Biotechnology* **11**, 7 (2011).
5. S. Schmollinger, *et al.*, Nitrogen-Sparing Mechanisms in *Chlamydomonas* Affect the Transcriptome, the Proteome, and Photosynthetic Metabolism. *The Plant Cell* **26**, 1410–1435 (2014).
6. M. T. Juergens, *et al.*, The Regulation of Photosynthetic Structure and Function during Nitrogen Deprivation in *Chlamydomonas reinhardtii*. *Plant Physiology* **167**, 558–573 (2015).
7. M. Schulz-Raffelt, *et al.*, Hyper-accumulation of starch and oil in a *Chlamydomonas* mutant affected in a plant-specific DYRK kinase. *Biotechnology for Biofuels* **9**, 55 (2016).
8. Y.-M. Zhang, H. Chen, C.-L. He, Q. Wang, Nitrogen Starvation Induced Oxidative Stress in an Oil-Producing Green Alga *Chlorella sorokiniana* C3. *PLOS ONE* **8**, e69225 (2013).
9. J.-J. Park, *et al.*, The response of *Chlamydomonas reinhardtii* to nitrogen deprivation: a systems biology analysis. *The Plant Journal* **81**, 611–624 (2015).
10. M. Gargouri, P. D. Bates, J.-J. Park, H. Kirchhoff, D. R. Gang, Functional photosystem I maintains proper energy balance during nitrogen depletion in *Chlamydomonas reinhardtii*, promoting triacylglycerol accumulation. *Biotechnology for Biofuels* **10**, 89 (2017).
11. Z.-Y. Du, *et al.*, Galactoglycerolipid Lipase PGD1 Is Involved in Thylakoid Membrane Remodeling in Response to Adverse Environmental Conditions in *Chlamydomonas*. *The Plant Cell* **30**, 447–465 (2018).
12. Q.-G. Tran, *et al.*, Impairment of starch biosynthesis results in elevated oxidative stress and autophagy activity in *Chlamydomonas reinhardtii*. *Sci Rep* **9**, 9856 (2019).
13. J. F. Allen, Cyclic, pseudocyclic and noncyclic photophosphorylation: new links in the chain. *Trends in Plant Science* **8**, 15–19 (2003).

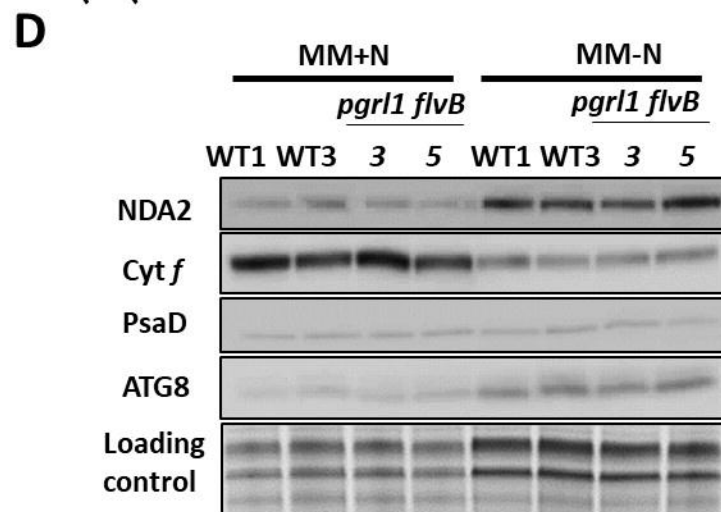
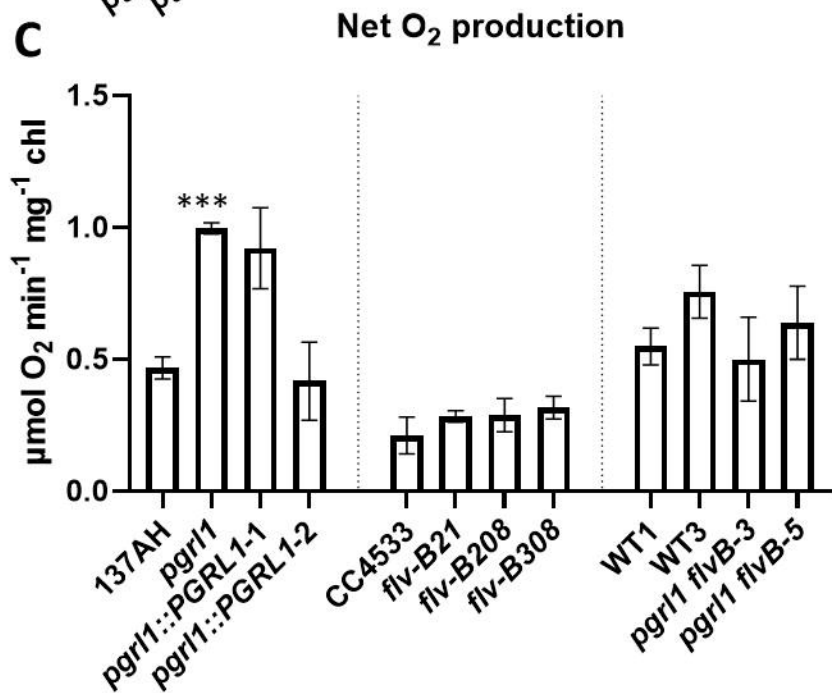
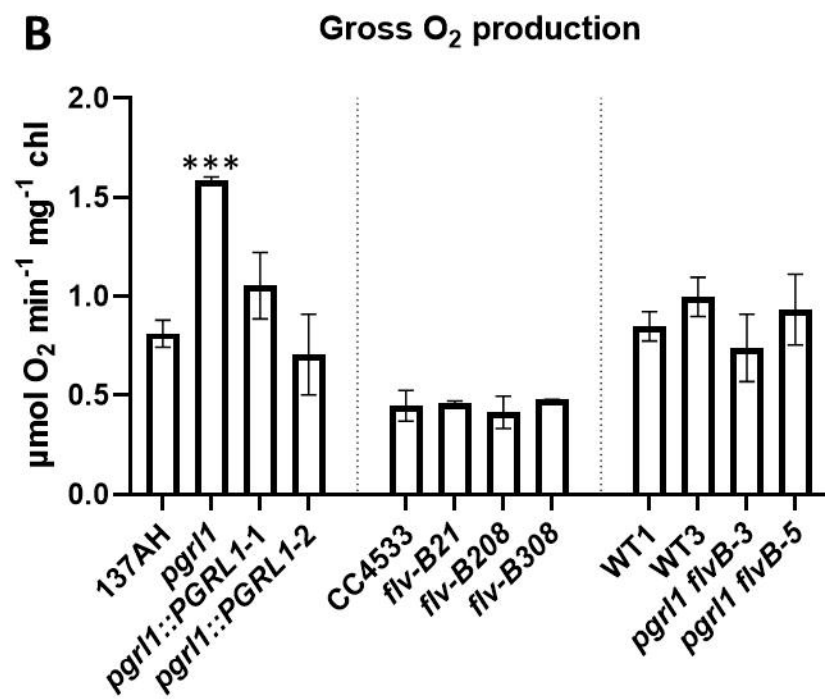
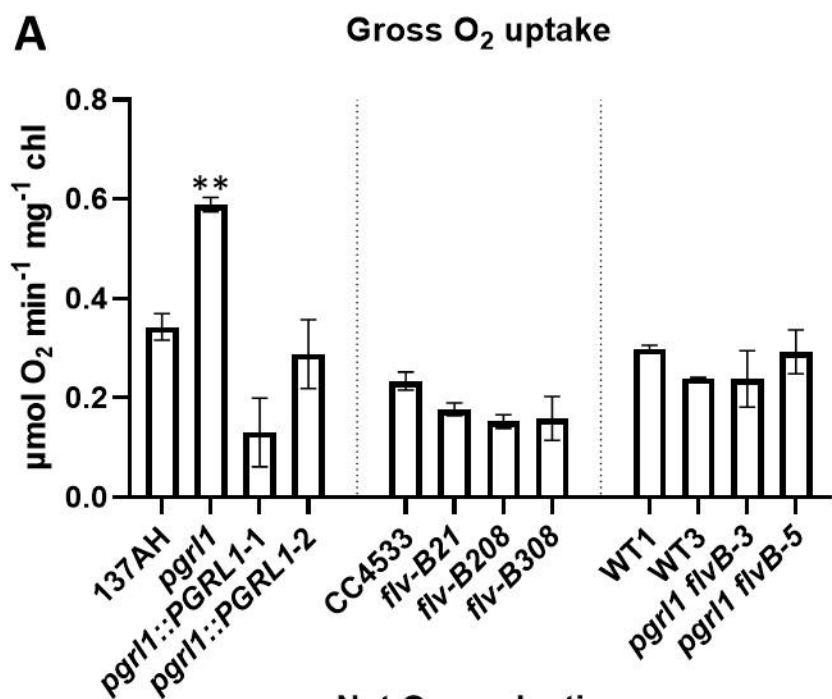
14. K.-V. Dang, *et al.*, Combined Increases in Mitochondrial Cooperation and Oxygen Photoreduction Compensate for Deficiency in Cyclic Electron Flow in *Chlamydomonas reinhardtii*. *The Plant Cell* **26**, 3036–3050 (2014).
15. B. Bailleul, *et al.*, Energetic coupling between plastids and mitochondria drives CO₂ assimilation in diatoms. *Nature* **524**, 366–369 (2015).
16. A. Burlacot, G. Peltier, Y. Li-Beisson, Subcellular Energetics and Carbon Storage in *Chlamydomonas*. *Cells* **8**, 1154 (2019).
17. S. Saroussi, *et al.*, Alternative outlets for sustaining photosynthetic electron transport during dark-to-light transitions. *Proc Natl Acad Sci USA* **116**, 11518–11527 (2019).
18. C. Desplats, *et al.*, Characterization of Nda2, a Plastoquinone-reducing Type II NAD(P)H Dehydrogenase in *Chlamydomonas* Chloroplasts. *J. Biol. Chem.* **284**, 4148–4157 (2009).
19. D. Tolleter, *et al.*, Control of Hydrogen Photoproduction by the Proton Gradient Generated by Cyclic Electron Flow in *Chlamydomonas reinhardtii*[W]. *Plant Cell* **23**, 2619–2630 (2011).
20. A. P. Hertle, *et al.*, PGRL1 Is the Elusive Ferredoxin-Plastoquinone Reductase in Photosynthetic Cyclic Electron Flow. *Molecular Cell* **49**, 511–523 (2013).
21. Y. Munekage, *et al.*, PGR5 Is Involved in Cyclic Electron Flow around Photosystem I and Is Essential for Photoprotection in *Arabidopsis*. *Cell* **110**, 361–371 (2002).
22. S. I. Saroussi, T. M. Wittkopp, A. R. Grossman, The Type II NADPH Dehydrogenase Facilitates Cyclic Electron Flow, Energy-Dependent Quenching, and Chlororespiratory Metabolism during Acclimation of *Chlamydomonas reinhardtii* to Nitrogen Deprivation. *Plant Physiology* **170**, 1975–1988 (2016).
23. C. Gerotto, *et al.*, Flavodiiron proteins act as safety valve for electrons in *Physcomitrella patens*. *PNAS* **113**, 12322–12327 (2016).
24. F. Chaux, *et al.*, Flavodiiron Proteins Promote Fast and Transient O₂ Photoreduction in *Chlamydomonas*. *Plant Physiology* **174**, 1825–1836 (2017).
25. A. Burlacot, *et al.*, Alternative photosynthesis pathways drive the algal CO₂-concentrating mechanism. *Nature*, 1–6 (2022).
26. J. F. Allen, Photosynthesis of ATP—Electrons, Proton Pumps, Rotors, and Poise. *Cell* **110**, 273–276 (2002).
27. G. Peers, *et al.*, An ancient light-harvesting protein is critical for the regulation of algal photosynthesis. *Nature* **462**, 518–521 (2009).
28. G. Bonente, *et al.*, Analysis of LhcSR3, a Protein Essential for Feedback De-Excitation in the Green Alga *Chlamydomonas reinhardtii*. *PLOS Biology* **9**, e1000577 (2011).
29. E. Erickson, S. Wakao, K. K. Niyogi, Light stress and photoprotection in *Chlamydomonas reinhardtii*. *The Plant Journal* **82**, 449–465 (2015).
30. H. H. Stiehl, H. T. Witt, Quantitative treatment of the function of plastoquinone in photosynthesis. *Z Naturforsch B* **24**, 1588–1598 (1969).
31. C. Foyer, R. Furbank, J. Harbinson, P. Horton, The mechanisms contributing to photosynthetic control of electron transport by carbon assimilation in leaves. *Photosynth Res* **25**, 83–100 (1990).
32. Y. Munekage, *et al.*, Cytochrome b6f mutation specifically affects thermal dissipation of absorbed light energy in *Arabidopsis*. *The Plant Journal* **28**, 351–359 (2001).
33. M. Jokel, *et al.*, *Chlamydomonas* Flavodiiron Proteins Facilitate Acclimation to Anoxia During Sulfur Deprivation. *Plant and Cell Physiology* **56**, 1598–1607 (2015).
34. M. Jokel, X. Johnson, G. Peltier, E.-M. Aro, Y. Allahverdiyeva, Hunting the main player enabling *Chlamydomonas reinhardtii* growth under fluctuating light. *The Plant Journal* **94**, 822–835 (2018).
35. H. Chen, *et al.*, Ca²⁺-regulated cyclic electron flow supplies ATP for nitrogen starvation-induced lipid biosynthesis in green alga. *Sci Rep* **5**, 15117 (2015).
36. F. Kong, *et al.*, Interorganelle Communication: Peroxisomal MALATE DEHYDROGENASE2 Connects Lipid Catabolism to Photosynthesis through Redox Coupling in *Chlamydomonas*. *The Plant Cell* **30**, 1824–1847 (2018).

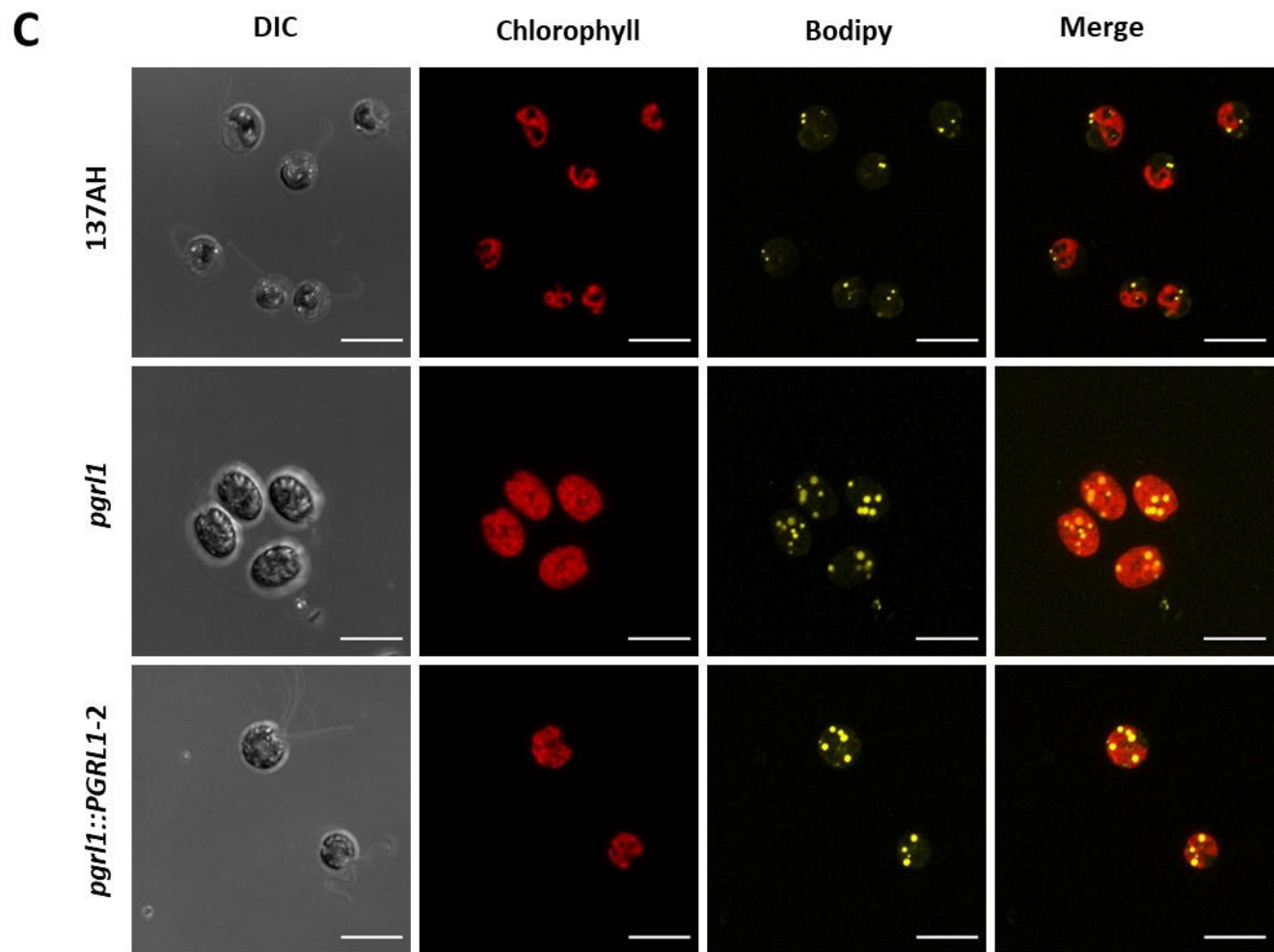
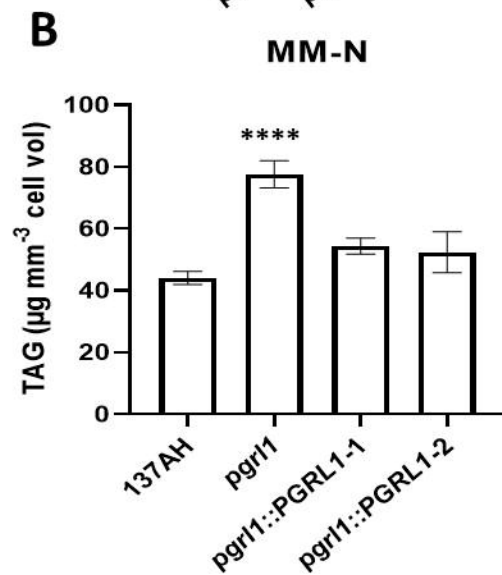
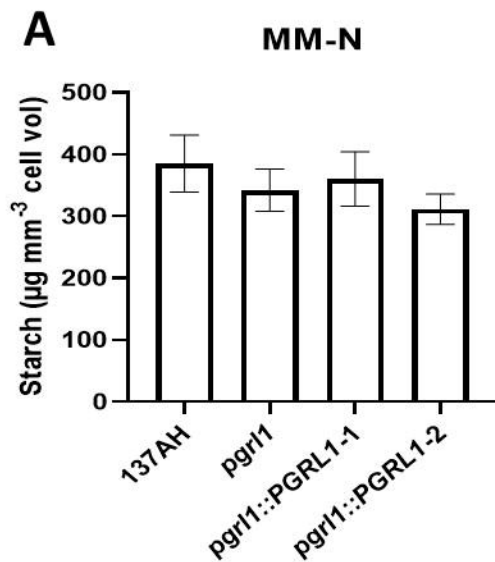
37. S. Wu, *et al.*, Elevated CO₂ improves both lipid accumulation and growth rate in the glucose-6-phosphate dehydrogenase engineered *Phaeodactylum tricornutum*. *Microb Cell Fact* **18** (2019).
38. G. Peltier, G. W. Schmidt, Chlororespiration: an adaptation to nitrogen deficiency in *Chlamydomonas reinhardtii*. *Proceedings of the National Academy of Sciences* **88**, 4791–4795 (1991).
39. L. Bulté, F.-A. Wollman, Evidence for a selective destabilization of an integral membrane protein, the cytochrome b₆/f complex, during gametogenesis in *Chlamydomonas reinhardtii*. *European Journal of Biochemistry* **204**, 327–336 (1992).
40. A. Burlacot, *et al.*, Flavodiiron-Mediated O₂ Photoreduction Links H₂ Production with CO₂ Fixation during the Anaerobic Induction of Photosynthesis. *Plant Physiol.* **177**, 1639–1649 (2018).
41. S. Saroussi, E. Sanz-Luque, R. G. Kim, A. R. Grossman, Nutrient scavenging and energy management: acclimation responses in nitrogen and sulfur deprived *Chlamydomonas*. *Current Opinion in Plant Biology* **39**, 114–122 (2017).
42. K. Sonoike, I. Terashima, Mechanism of photosystem-I photoinhibition in leaves of *Cucumis sativus* L. *Planta* **194**, 287–293 (1994).
43. G. DalCorso, *et al.*, A complex containing PGRL1 and PGR5 is involved in the switch between linear and cyclic electron flow in *Arabidopsis*. *Cell* **132**, 273–285 (2008).
44. J. E. Johnson, J. A. Berry, The role of Cytochrome b₆f in the control of steady-state photosynthesis: a conceptual and quantitative model. *Photosynth Res* **148**, 101–136 (2021).
45. S. Saroussi, *et al.*, Reversible restriction of electron flow across cytochrome b₆f in dark acclimated cells limited for downstream electron sinks. 2022.10.04.507358 (2022).
46. H. Yamamoto, T. Shikanai, PGR5-Dependent Cyclic Electron Flow Protects Photosystem I under Fluctuating Light at Donor and Acceptor Sides. *Plant Physiology* **179**, 588–600 (2019).
47. D. Petroutsos, *et al.*, PGRL1 Participates in Iron-induced Remodeling of the Photosynthetic Apparatus and in Energy Metabolism in *Chlamydomonas reinhardtii**. *Journal of Biological Chemistry* **284**, 32770–32781 (2009).
48. X. Johnson, *et al.*, Proton Gradient Regulation 5-Mediated Cyclic Electron Flow under ATP- or Redox-Limited Conditions: A Study of Δ ATPase *pgr5* and Δ rbcl *pgr5* Mutants in the Green Alga *Chlamydomonas reinhardtii* 1[C][W]. *Plant Physiol* **165**, 438–452 (2014).
49. J. Steinbeck, *et al.*, Deletion of Proton Gradient Regulation 5 (PGR5) and PGR5-Like 1 (PGRL1) proteins promote sustainable light-driven hydrogen production in *Chlamydomonas reinhardtii* due to increased PSII activity under sulfur deprivation. *Front Plant Sci* **6**, 892 (2015).
50. F. Buchert, L. Mosebach, P. Gäbelein, M. Hippler, PGR5 is required for efficient Q cycle in the cytochrome b₆f complex during cyclic electron flow. *Biochemical Journal* **477**, 1631–1650 (2020).
51. C. A. Sacksteder, A. Kanazawa, M. E. Jacoby, D. M. Kramer, The proton to electron stoichiometry of steady-state photosynthesis in living plants: A proton-pumping Q cycle is continuously engaged. *Proc Natl Acad Sci U S A* **97**, 14283–14288 (2000).
52. W. A. Cramer, S. S. Hasan, E. Yamashita, The Q Cycle of Cytochrome bc Complexes: a Structure Perspective. *Biochim Biophys Acta* **1807**, 788–802 (2011).
53. G. Finazzi, J. Minagawa, G. N. Johnson, “The Cytochrome b₆f Complex: A Regulatory Hub Controlling Electron Flow and the Dynamics of Photosynthesis?” in *Cytochrome Complexes: Evolution, Structures, Energy Transduction, and Signaling*, Advances in Photosynthesis and Respiration., W. A. Cramer, T. Kallas, Eds. (Springer Netherlands, 2016), pp. 437–452.
54. S. Wada, *et al.*, Flavodiiron Protein Substitutes for Cyclic Electron Flow without Competing CO₂ Assimilation in Rice. *Plant Physiology* **176**, 1509–1518 (2018).
55. L. Basso, K. Sakoda, R. Kobayashi, W. Yamori, T. Shikanai, Flavodiiron proteins enhance the rate of CO₂ assimilation in *Arabidopsis* under fluctuating light intensity. *Plant Physiology*, kiac064 (2022).

56. R. Miller, *et al.*, Changes in Transcript Abundance in *Chlamydomonas reinhardtii* following Nitrogen Deprivation Predict Diversion of Metabolism1[W][OA]. *Plant Physiol* **154**, 1737–1752 (2010).
57. I. K. Blaby, *et al.*, Systems-level analysis of nitrogen starvation-induced modifications of carbon metabolism in a *Chlamydomonas reinhardtii* starchless mutant. *Plant Cell* **25**, 4305–4323 (2013).
58. K. Zienkiewicz, Z.-Y. Du, W. Ma, K. Vollheyde, C. Benning, Stress-induced neutral lipid biosynthesis in microalgae — Molecular, cellular and physiological insights. *Biochimica et Biophysica Acta (BBA) - Molecular and Cell Biology of Lipids* **1861**, 1269–1281 (2016).
59. T. Takeuchi, C. Benning, Nitrogen-dependent coordination of cell cycle, quiescence and TAG accumulation in *Chlamydomonas*. *Biotechnology for Biofuels* **12**, 292 (2019).
60. F. Kong, Y. Yamaoka, T. Ohama, Y. Lee, Y. Li-Beisson, Molecular Genetic Tools and Emerging Synthetic Biology Strategies to Increase Cellular Oil Content in *Chlamydomonas reinhardtii*. *Plant Cell Physiol* **60**, 1184–1196 (2019).
61. Y. Li-Beisson, J. J. Thelen, E. Fedosejevs, J. L. Harwood, The lipid biochemistry of eukaryotic algae. *Progress in Lipid Research* **74**, 31–68 (2019).
62. P. Geigenberger, A. Kolbe, A. Tiessen, Redox regulation of carbon storage and partitioning in response to light and sugars. *Journal of Experimental Botany* **56**, 1469–1479 (2005).
63. L. Michelet, *et al.*, Redox regulation of the Calvin–Benson cycle: something old, something new. *Front Plant Sci* **4** (2013).
64. P. Geigenberger, A. R. Fernie, Metabolic Control of Redox and Redox Control of Metabolism in Plants. *Antioxid Redox Signal* **21**, 1389–1421 (2014).
65. X. Li, *et al.*, A Galactoglycerolipid Lipase Is Required for Triacylglycerol Accumulation and Survival Following Nitrogen Deprivation in *Chlamydomonas reinhardtii*. *The Plant Cell* **24**, 4670–4686 (2012).
66. H. Chen, *et al.*, Ca²⁺-regulated cyclic electron flow supplies ATP for nitrogen starvation-induced lipid biosynthesis in green alga. *Sci Rep* **5**, 15117 (2015).
67. X. Johnson, J. Alric, Interaction between Starch Breakdown, Acetate Assimilation, and Photosynthetic Cyclic Electron Flow in *Chlamydomonas reinhardtii*. *J. Biol. Chem.* **287**, 26445–26452 (2012).
68. X. Johnson, J. Alric, Central Carbon Metabolism and Electron Transport in *Chlamydomonas reinhardtii*: Metabolic Constraints for Carbon Partitioning between Oil and Starch. *Eukaryot Cell* **12**, 776–793 (2013).
69. M. Saint-Sorny, P. Brzezowski, S. Arrivault, J. Alric, X. Johnson, Interactions Between Carbon Metabolism and Photosynthetic Electron Transport in a *Chlamydomonas reinhardtii* Mutant Without CO₂ Fixation by RuBisCO. *Frontiers in Plant Science* **13** (2022).
70. C. Goodson, R. Roth, Z. T. Wang, U. Goodenough, Structural correlates of cytoplasmic and chloroplast lipid body synthesis in *Chlamydomonas reinhardtii* and stimulation of lipid body production with acetate boost. *Eukaryot Cell* **10**, 1592–1606 (2011).
71. U. Goodenough, *et al.*, The path to triacylglyceride obesity in the sta6 strain of *Chlamydomonas reinhardtii*. *Eukaryot Cell* **13**, 591–613 (2014).
72. K. Maxwell, G. N. Johnson, Chlorophyll fluorescence—a practical guide. *J Exp Bot* **51**, 659–668 (2000).
73. A. Burlacot, F. Burlacot, Y. Li-Beisson, G. Peltier, Membrane Inlet Mass Spectrometry: A Powerful Tool for Algal Research. *Front Plant Sci* **11**, 1302 (2020).











— 137AH
— *pgrl1*

Legend:

